Experimental Characterization of Ethyl Acetate, Ethyl Propionate, and Ethyl Butanoate in a Homogeneous Charge Compression Ignition Engine

ARTICLE *in* ENERGY & FUELS · MARCH 2011

Impact Factor: 2.79 · DOI: 10.1021/ef101602q

4 AUTHORS:

Francesco Contino
Vrije Universiteit Brussel
46 PUBLICATIONS **165** CITATIONS
SEE PROFILE

F. Foucher
Université d'Orléans
118 PUBLICATIONS **736** CITATIONS
SEE PROFILE

Christine Mounaïm-Rousselle
Université d'Orléans
104 PUBLICATIONS **1,068** CITATIONS
SEE PROFILE

Hervé Jeanmart
Université catholique de Louvain
65 PUBLICATIONS **534** CITATIONS
SEE PROFILE

Experimental characterization of ethyl acetate, ethyl propionate and ethyl butanoate in a HCCI engine

Francesco Contino,*,† Fabrice Foucher,‡ Christine Mounaïm-Rousselle,‡ and Hervé Jeanmart†

Université catholique de Louvain, Institute of Mechanics, Materials, and Civil Engineering, Louvain-la-Neuve, Belgium, and Université d'Orléans, Institut Prisme, Orléans, France

E-mail: francesco.contino@uclouvain.be

Abstract

The Homogeneous Charge Compression Ignition (HCCI) engine can be run on a large range of fuels if the appropriate operating conditions are chosen. This can improve the efficiency of biofuels production from low-value biomass by suppressing the need for the transformation process to obtain products that are compatible with spark ignition or compression ignition engines. A simple biochemical process that includes acidogenic fermentation and produces a mixture of various esters, can take advantage of this flexibility. However, the behavior of this mixture under HCCI conditions need to be characterized. It can also have a great impact on the HCCI operating limits and its successful implementation. Using a HCCI engine, we investigated how the operating limits are modified by the combustion characteristics of three of these esters: ethyl acetate, ethyl propionate and ethyl butanoate. This paper reports the experimental results for each of these products and for ethanol taken as the reference fuel. It also

*To whom correspondence should be addressed

†Université catholique de Louvain, Institute of Mechanics, Materials, and Civil Engineering, Louvain-la-Neuve, Belgium

‡Université d'Orléans, Institut Prisme, Orléans, France

analyzes their effects on the ignition timing and the combustion rate. For the selected operating conditions, stable HCCI operations on a large range of equivalence ratios were obtained for every fuels. The difference in specific heats of the air/fuel mixtures and in the ignition kinetics both contributed to the ignition characteristics. Ethanol ignites earlier which lead to a low upper limit while the late ignition of ethyl acetate shifts the operating zone upward due to smoothed high loads but unstable low loads. As a consequence, these low-grade products can be used on a HCCI engine. Fuel blends of these products may take advantage of the different combustion characteristics to extend the HCCI zone. Still, the range of this extension is difficult to estimate and the research of the optimal fuel blend composition will therefore remain the focus of future work.

Introduction

The production of biofuels is constrained by the specific fuel characteristics required for spark ignition (SI) and compression ignition (CI) engines. Therefore, a great part of the biomass energy content is lost in the successive conversions steps, hence decreasing the overall energy balance, e.g. the production of ethanol from corn, sugar beet or wheat consume up to 85% of the ethanol energy output[1,2].

The Homogeneous Charge Compression Ignition (HCCI) engine not only offers a great potential of efficiency improvement and emissions reduction (i.e. NOx and soot)[3–6] but it can also be run on any type of fuel given that the appropriate operating conditions are chosen[7–10].

This flexibility allows the use of low-grade fuels as transportation fuels. It gives an opportunity to develop more simple and more efficient bioconversion processes, as illustrated by Mack et al. with the use of wet-ethanol[11].

Products resulting from acidogenic fermentation (acidogenesis) will be further discussed in this paper. Acidogenesis is traditionally considered to decrease negative ecological effects of polluting compounds. This process can be extended to low-value biomass wastes to allow their conversion into useful organic compounds. It produces volatile organic acids (including acetic, propionic, butyric and lactic acids) and has three main advantages compared to ethanol fermentation[12,13]: source diversification, efficiency and easy implementation. Indeed, it can use not only sugar but a wide range of fermentable organic substrates poorly or not treated (e.g. organic wastes). Less treatment to hydrolyze biomass is required because acidogenic bacteria have hydrolysis capacity while yeast does not. Moreover, acidogenic fermentation does not require a germ free environment.

Although the volatile organic acids could be directly used in an engine, it is generally not considered due to materials resistance. Therefore, they are partly combined with ethanol (produced during the first stages of the acidogenic fermentation) and the remaining part can be combined with glycerol, offering a market for this by-product of the biodiesel production[14–16]. This process leads to a large range of esters from ethyl acetate ($C_4H_8O_2$) to tributyrin ($C_{15}H_{26}O_6$).

Alternative fuels are an opportunity to widen the HCCI zone, i.e. the range of load and speed

where HCCI combustion is possible[17]. The heat released is mainly controlled by the ignition timing and the combustion duration. It is, therefore, important to understand how these parameters are related to the particular fuel properties. In a previous work, we have studied numerically the HCCI running zone using ethyl acetate[18]. It was shown that ethyl acetate has a similar running area than iso-octane but it is shifted towards upper charges. This indicates that ethyl acetate is more resistant to ignition than iso-octane.

In this paper, three of the esters obtained by acidogenesis are analyzed experimentally on a HCCI engine : ethyl acetate (EtAc), ethyl propionate (EtPr) and ethyl butanoate (EtBu). The objective is to understand their behavior under HCCI conditions. These results will also be used in future studies to characterize a fuel blend of these products and will suggest how to adjust the fermentation toward the optimal fuel blend composition.

Combustion of EtAc, EtPr and EtBu have already been investigated in the context of biodiesel characterization[19–22]. These studies focused on a better understanding of the mechanism of oxygenates combustion to extend it to biodiesel, mainly composed of long chain fatty esters. EtAc combustion has also been studied in the context of thermal oxidizers for reducing the pollution of volatile organic compounds[23].

This paper first describes the experimental setup. It then presents the results of the experiments on the three esters taking ethanol (EtOH) as the reference fuel. Finally, it discusses how the combustion characteristics alter the operating zone.

Experimental setup

This section first introduces the characteristics of the fuels. It then describes the details of the engine and finally discusses the experimental procedure.

Fuels characteristics

The fuels used in the experiments are esters resulting from the reaction of volatile organic acids (acetic, propionic and butanoic acids) with ethanol.

The three esters have similar ignition points (or autoignition temperature measured with the procedure described in the ASTM E659 and given in the material safety data sheet), around 450°C, which is 90°C above ethanol. Even if the method to determine this temperature is different from the HCCI conditions, it indicates that ethanol should ignite more rapidly. Moreover, within the esters, even if the ignition points are not significantly different, EtBu have probably a shorter ignition delay because of its longer chain.

The lower heating value (LHV) of all four fuels are significantly smaller than petroleum-based fuels due to their oxygenated nature. However, the air/fuel mixtures have similar energy content for the same equivalence ratio resulting in no loss of power (see Table 1).

The esters have a significantly lower energy of vaporization than ethanol and only slightly higher than those of gasoline and diesel. This would have a positive impact for the mixture preparation on a real engine. In the following experiments, the vaporization energy is, however, not relevant because the fuel/air mixture is prepared externally in a fuel vaporizer (see next section).

Engine details and data acquisition

The engine is based on the PSA DW10 model that has a displacement of 0.499 liters per cylinder. It is converted to single-cylinder and mounted on a electric motor that can maintain a constant revolution speed. The geometric compression ratio is 15.35 and the effective compression ratio evaluated by the method described by Tazerout et al.[24] is 14.15. The specifications of the engine are listed in Table 2.

The intake air is supplied by an air compressor and is electrically heated to the desired set point. It is metered and controlled by a Brooks 5853S model to obtain an intake pressure of 1.5 bar in the intake plenum.

The fuel flow from a pressurized tank is metered and controlled by a Bronkhorst M13 Coriolis

flow sensor. Fuel is fully premixed with the intake air by supplying a fuel/air mixture from the heated fuel-vaporization chamber upstream of the intake plenum. This plenum is designed to minimize the pressure oscillations and to improve the mixture homogeneity.

The intake conditions are measured in the intake manifold by a Kistler 4075A piezoresistive absolute pressure sensor ($\pm$3 kPa) and by two K thermocouples ($\pm$2 K) in both intake ducts just above the inlet valves.

Cylinder pressure measurements are made with a Kistler 6043A piezoelectric transducer ($\pm$2% of the measured value) at 0.1 crank angle degrees (CAD) increments. The piezoelectric transducer offset is determined by the mean value of the absolute pressure in the intake manifold at the end of the intake stroke when the pressure is stabilized.

The temperatures of the cooling water and the lubricating oil were held constant during the experiments at a value of 93°C and 90°C respectively.

The emissions are measured by an Environnement S.A. exhaust gas analyzer. The overall precision is 1% of the full scale output (FSO). This analyzer is made up of the Topaze 32M model for NO_x measurements (FSO: 1%), the Graphite 52M model for unburnt hydrocarbon (uHC, FSO: 1%) and CH4 measurements (FSO: 1000ppm), and the Mir2M model for CO (separated high and low range, FSO: 10% and 2000ppm), CO2 and O2 (FSO : 25%) measurements.

A schematic of the experimental setup is shown in Figure 1.

Experimental procedure

As the main objective is to understand the behavior of each fuel and apply these results in future studies to characterize a fuel blend, these products are compared at the same intake conditions. We held constant the settings of the temperature after the heater (270°C) and the pressure in the intake plenum (1.5 bar). The operating regions were therefore not optimized for each fuel but the focus is on the impact of each fuel on the operating zone.

Two engine speeds have been investigated: 1000 and 1500 rpm. Due to small differences in heat transfer after the heater, the temperatures in the intake manifold were 230°C and 235°C for

1000 and 1500 rpm respectively.

Pressure data from 100 consecutive cycles were stored and analyzed by the data acquisition system when combustion was stabilized. Among the parameters calculated on each cycle were: the maximum pressure (P_{max}), the crank angle at which P_{max} occured, the maximum pressure rise rate (MPRR) and the indicated mean effective pressure (IMEP). The mean values and standard deviations of these parameters based on 100 cycles were calculated online and used to determine stabilization and operating limits. These values were also used to compute the coefficient of variation of IMEP (CoV_{IMEP}), given by the standard deviation of IMEP divided by its mean.

We adjusted the fuel injection to modify the equivalence ratio until we went past one of the HCCI limits. These limits were defined for this work as a maximum MPRR of 7 bar/CAD for the upper or knock limit and a maximum CoV_{IMEP} of 5% for the lower or misfire limit.

The reported mass-averaged temperatures are computed using the ideal gas law in combination with the measured pressure, the known cylinder volume and the temperature at bottom dead center (T_{BDC}). Several effects should be considered when computing T_{BDC}[25] : mixing with residuals, heat-transfer, gas dynamic effects and vaporization of directly injected liquid fuel. However, the trapped residuals were small due to the pressurized inlet and the atmospheric exhaust; the air/fuel mixture was prepared externally without any vaporization in the cylinder; and the gas dynamic effects were not considered since the two investigated engine speeds were close and small. Therefore, we considered that T_{BDC} was equal to the temperature measured just before the inlet valves. This is a good approximation when comparing the fuels on the same engine with the same settings.

The heat release rate (HRR) was computed from the cylinder-pressure data and the cylinder volume:

$$\frac{dQ}{d\theta} = \frac{C_p}{R} p \frac{dV}{d\theta} + \frac{C_V}{R} V \frac{dp}{d\theta} + Q_{\text{wall}}, \tag{1}$$

where θ is the crank angle, C_p and C_V are the specific heats at constant pressure and constant volume respectively, R the ideal gas constant, p the pressure, V the volume of the combustion chamber and Q_{wall} the wall heat transfer. The wall heat transfer is modeled by the Hohenberg

correlation[26]. This correlation has been shown to give very good results for HCCI engines[27]. The specific heats are computed from the JANAF tables and include the change of composition due to the combustion with a two steps algorithm. First, they are arbitrarily modified at top dead center (TDC) from the composition of the air/fuel mixture to the composition of the complete combustion products. The cumulative heat release is then computed from the HRR obtained with eq. (1). As this change of specific heats is arbitrary, a second step use the cumulative heat release normalized by its maximum as a conversion factor between reactants and products and a better approximation of the heat release rate is obtained.

To characterize the combustion, three parameters were calculated for each cycle: CA10, CA50 and CA90. They correspond to the points where 10%, 50% and 90% of the the cumulative heat release was reached respectively. CA10 is a good indicator of the combustion start for single-stage fuels, as in this work. CA50 is often used to monitor the combustion and adjust the inlet conditions. The difference between CA90 and CA10 defines the combustion duration. The uncertainties on these parameters come from the uncertainty on HRR which is due to the precision of the pressure sensor, the error on the effective compression ratio and the assumptions of the heat transfer model. According to the slope of the cumulative heat release curve which increases with increasing equivalence ratio, they have been evaluated between ± 1 CAD for an equivalence ratio of 0.08 and ± 0.2 CAD for an equivalence ratio of 0.4.

Results

This section first compares the impact of the combustion characteristics on the operating ranges of EtAc, EtPr, EtBu and EtOH. It then presents the emissions and finally analyzes the ignition delays of these products.

Operating zone

As discussed in the previous section, the inlet conditions were kept constant. They were chosen so that most of the CA50 are in the narrow range where an HCCI engine can be operated[28]: -5 to 10 crank angle degrees after top dead center (CAD ATDC) as shown in Figure 2.

The fuels exhibit quite different combustion characteristics (see Figure 3).

EtOH ignites well before TDC which leads to very high MPRR at equivalence ratios above 0.20. EtAc ignites much more later bringing issues for the instability at equivalence ratios below 0.20. EtPr ignites later than EtBu but both are in the region where a large range of equivalence ratios can be used without reaching a HCCI limit. These differences have a great impact on the operating zones (see Figure 4). Due to the early ignition of EtOH, the combustion is very stable reaching the lower limit at a very low equivalence ratio below 0.08. But the MPRR is increasing quickly with the equivalence ratio, reaching the upper limit at around 3 bar. EtBu ignites more slowly which increases the upper limit but without changing the instability limit. For these settings, EtPr has a high upper limit around 5 bar while keeping a similar lower limit. The late ignition of EtAc leads to a smoother pressure rise rate. Consequently, the upper limit is around 6.5 bar. However, this also leads to more instability which increases the lower limit at around 2 bar.

When reaching the misfire limit the combustion is unstable and products of incomplete combustion increase. The CO and uHC emissions are thus related to the position in the HCCI zone. They significantly increase with decreasing equivalence ratio and reach a plateau near the misfire limit (see Figure 5).

The NO_x emissions correspond to the very low levels commonly obtained in HCCI engines[17], with a peak around 50 ppm for the highest IMEP achieved with EtAc.

Ignition delay and combustion duration

The products tested are single-stage fuels. The difference of combustion characteristics is, therefore, mainly due to different ignition delays. These ignition delays were characterized by the CA10 computed for each cycle. In the specified conditions, EtOH had the shortest ignition delay

followed by EtBu, EtPr and EtAc (see Figure 6 for all the experiments). In Figure 6, CA10 of EtAc at 1500 rpm and equivalence ratios between 0.34 and 0.38 are above the other points due to a slightly lower inlet temperature (230°C instead of 235°C for the other points). This also explains the higher HCCI zone for EtAc at 1500 rpm shown in Figure 4.

The difference in ignition delays shown in Figure 6 is due not only to the intrinsic ignition kinetics but also to the different temperature histories. Each fuel has a different reaction path that leads to different ignition delays. Another major parameter is the ratio of specific heat of the air/fuel mixture. For the same equivalence ratio, the ratio of specific heats is higher for EtOH and smaller for EtAc. As the inlet conditions were held constant, the difference in the ratios of specific heats is illustrated by the difference of temperature before ignition (see the temperature at 15 CAD BTDC in Figure 7, the experimental variations of the inlet conditions are included in this figure). This will change the temperature history and therefore modify the ignition timing. These two effects are combined in the HCCI engine and both contribute to the difference between the fuels.

The effects of the reaction paths and the specific heats are also illustrated by the change of the ignition delay with the equivalence ratio. At low temperatures (below 1000 K) the alkylperoxy radical isomerization reactions control ignition and are faster for rich mixtures. Therefore for the same temperature, the ignition delay should decrease with increasing equivalence ratio. However, with more fuel in the mixture, the specific heats increase which reduce the ratio of specific heats and the resulting temperature before TDC (see Figure 7). Here, the thermal effect balances the kinetics effect which explains that CA10 does not change substantially with the equivalence ratio, see Figure 6.

To isolate the thermal effect, we ran ignition delay simulations using the Cosilab software[29]. We used the ethanol mechanism developed by Saxena and Williams[30], the ethyl acetate mechanism of Gasnot et al.[23], the ethyl propionate mechanism of Metcalfe et al.[21] and the ethyl butanoate mechanism of Hakka et al.[22] The ignition delay was defined computationally as the time before the maximum rate of temperature rise in an adiabatic vessel with constant volume.

The simulations results confirm that for the same temperature (the temperature at 15 CAD BTDC for the lowest equivalence ratio of each fuel, see Figure 7), the ignition delay decreases with increasing equivalence ratio (see empty symbols in Figure 8). However, if the temperature is modified for each equivalence ratio according to the mass-averaged temperature at 15 CAD BTDC (see Figure 7), the thermal effect compensates the kinetics effect and the ignition delay remains approximately constant (see full symbols in Figure 8).

The combustion durations are quite similar and constant for all fuels at low equivalence ratio (around 13 CAD for equivalence ratios below 0.15). Then, they decrease to reach 5 CAD. For a given equivalence ratio, EtOH has the smallest duration and EtAc the longest. This smoothes the pressure rise rate of EtAc and explains the higher knock limit (see Figure 9). The combined effects of the ignition delays and the combustion durations are illustrated by the CA50 shown in Figure 2.

Conclusion

Ethyl acetate, ethyl propionate and ethyl butanoate (products obtained by acidogenic fermentation) can be used in a HCCI engine. They produce stable and smooth HCCI combustion for a large range of equivalence ratios. Compared to ethanol, these products ignite more slowly. For the given conditions, this increases the upper limit while the lower limit is unaffected for ethyl propionate and ethyl butanoate. For ethyl acetate, however, the lower limit is modified due to more instability.

The main objective of the acidogenic fermentation route is to produce transportation fuels from low-value biomass. It tries to reduce the number of conversion processes but also to minimize the energy-consuming separation processes. Therefore, future studies will focus on the differences of combustion characteristics of those products in a fuel blend. Our results invite to analyze whether this fuel blend could take advantage of these differences to extend the HCCI zone by promoting the ignition with EtBu and smoothing it with EtAc.

Acknowledgement

This research is supported by the F.R.S. - FNRS through a research fellowship. The authors would like to thank the following people from Institut Prisme for their help with this study: Bruno Moreau for assembling and maintaining the engine and Julien Lemaire for help with the exhaust gas analyser. The authors would also like to thank Dr. Charles K. Westbrook for his advices on oxidation kinetics.

References

(1) Edwards, R.; Griesemann, J.-C.; Larivé, J.-F.; Mahieu., V. *Well-To-Wheels Analysis of Future Automotive Fuels and Powertrains in the European Context*; EUCAR, CONCAWE and JRC, 2004.

(2) Cherubini, F.; Bird, N.; Cowie, A.; Jungmeier, G.; Schlamadinger, B.; Woess-Gallasch, S. *Resour Conserv Recy* **2009**, *53*, 434–447.

(3) Najt, P. M.; Foster, D. E. *SAE Paper* **1983**, *830264*.

(4) Thring, R. H. *SAE Paper* **1989**, *892068*.

(5) Zhao, H.; Li, J.; Ma, T.; Ladommatos, N. *SAE Paper* **2002**, *2002-01-0420*.

(6) Dec, J. E. *Proc. Combust. Inst.* **2009**, *32*, 2727–2742.

(7) Christensen, M.; Hultqvist, A.; Johansson, B. *SAE Paper* **1999**, *1999-01-3679*.

(8) Tanaka, S.; Ayala, F.; Keck, J. C.; Heywood, J. B. *Combust. Flame* **2003**, *132*, 219–239.

(9) Jeuland, N.; Montagne, X. *Oil & Gas Science and Technology - Rev. IFP* **2006**, *61*, 85–94.

(10) Risberg, P. Describing the auto-ignition quality of fuels in HCCI engines. Ph.D. thesis, KTH, 2006.

(11) Mack, J. H.; Aceves, S. M.; Dibble, R. W. *Energy* **2009**, *34*, 782–787.

(12) Kleerebezem, R.; van Loosdrecht, M. C. M. *Curr. Opin. Biotechnol.* **2007**, *18*, 207–212.

(13) Zigová, J.; Šturdík, E. *J. Ind. Microbiol. Biotechnol.* **2000**, *24*, 153–160.

(14) Fernando, S.; Adhikari, S.; Kota, K.; Bandi, R. *Fuel* **2007**, *86*, 2806 – 2809.

(15) Gonçalves, V. L.; Pinto, B. P.; Silva, J. C.; Mota, C. J. *Catal. Today* **2008**, *133-135*, 673–677.

(16) Jaecker-Voirol, A.; Durand, I.; Hillion, G.; Delfort, B.; Montagne, X. *Oil & Gas Science and Technology - Rev. IFP* **2008**, *63*, 395–404.

(17) Zhao, F.; Asmus, T. W.; Assanis, D. N.; Dec, J. E.; Eng, J. A.; Najt, P. M. *Hommogeneous Charge Compression Ignition (HCCI) Engines, Key research and development issues*; SAE, 2003.

(18) Contino, F.; Jeanmart, H. *SAE Paper* **2009**, *2009-01-0297*.

(19) Westbrook, C. K.; Pitz, W. J.; Westmoreland, P. R.; Dryer, F. L.; Chaos, M.; Osswald, P.; Kohse-Höinghaus, K.; Cool, T. A.; Wang, J.; Yang, B.; Hansen, N.; Kasper, T. *Proc. Combust. Inst.* **2009**, *32*, 221–228.

(20) Walton, S. M.; Wooldridge, M. S.; Westbrook, C. K. *Proc. Combust. Inst.* **2009**, *32*, 255–262.

(21) Metcalfe, W. K.; Togbé, C.; Dagaut, P.; Curran, H. J.; Simmie, J. M. *Combust. Flame* **2009**, *156*, 250–260.

(22) Hakka, M. H.; Bennadji, H.; Biet, J.; Yahyaoui, M.; Sirjean, B.; Warth, V.; Coniglio, L.; Herbinet, O.; Glaude, P. A.; Billaud, F.; Battin-Leclerc, F. *Int. J. Chem. Kinet.* **2010**, *42*, 226–252.

(23) Gasnot, L.; Decottignies, V.; Pauwels, J. *Fuel* **2005**, *84*, 505–518.

(24) Tazerout, M.; Corre, O. L.; Stouffs, P. *SAE Paper* **1999**, *1999-01-3509*.

(25) Sjöberg, M.; Dec, J. *SAE Paper* **2004**, *2004-01-1900*.

(26) Hohenberg, G. F. *SAE Paper* **1979**, *790825*.

(27) Soyhan, H.; Yasar, H.; Walmsley, H.; Head, B.; Kalghatgi, G.; Sorusbay, C. *Appl. Therm. Eng.* **2009**, *29*, 541–549.

(28) Kalghatgi, G. T.; Head, R. A. *Int. J. Engine Res.* **2006**, *7*, 215–236.

(29) Cosilab Software, Version 3.2.1. Rotexo-Softpredict-Cosilab GmbH & Co. KG, Germany: http://www.SoftPredict.com, 2010.

(30) Saxena, P.; Williams, F. A. *Proc. Combust. Inst.* **2007**, *31*, 1149 – 1156.

Table 1: Fuel characteristics

	EtAc $C_4H_8O_2$	EtPr $C_5H_{10}O_2$	EtBu $C_6H_{12}O_2$	EtOH C_2H_6O
AFR_{stoich}	7.85	8.8	9.52	9.00
Density [kg/l]	0.897	0.891	0.886	0.789
LHV [MJ/kg]	23.79	26.53	28.64	27.75
LHV [MJ/l]	21.34	23.64	25.38	21.89
Ignition [°C]	460	440	463	362
Flash point [°C]	-4	12	26	12
Boiling temp. @1 atm. [°C]	77	99	120	78
Vapour pres. @20°C [hPa]	124	58	17	79
Δh_{vap} @25°C [kJ/kg]	404	368	367	837
Mm [kg/kmol]	88.1	102	116	46.1
Stoich. energy content [$kJ/kg_{mixture}$]	2689	2707	2741	2774

Table 2: Engine details

Bore [mm]	85
Stroke [mm]	88
Displacement [cm^3/cyl.]	499
Connecting rod length [mm]	145
Geometric Compression ratio	15.35
Effective Compression ratio	14.15
Number of valves	4

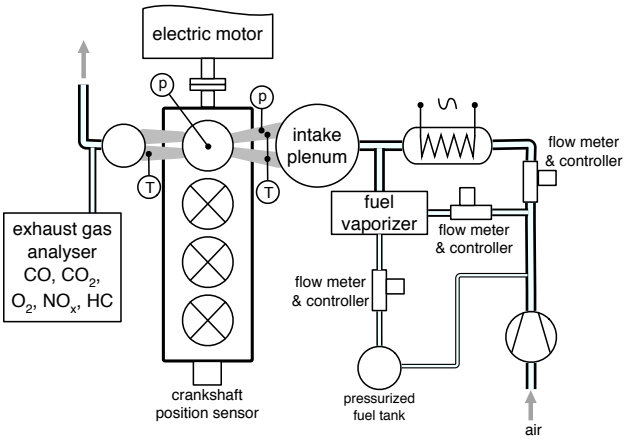

Figure 1: The engine is a PSA DW10 with a displacement of 499 cm^3/cyl converted to single-cylinder.

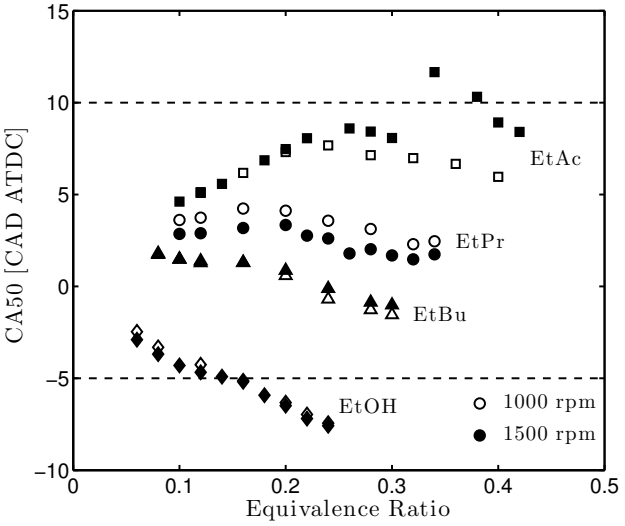

Figure 2: CA50 for the four fuels at 1000 rpm (empty symbols) and 1500 rpm (full symbols).

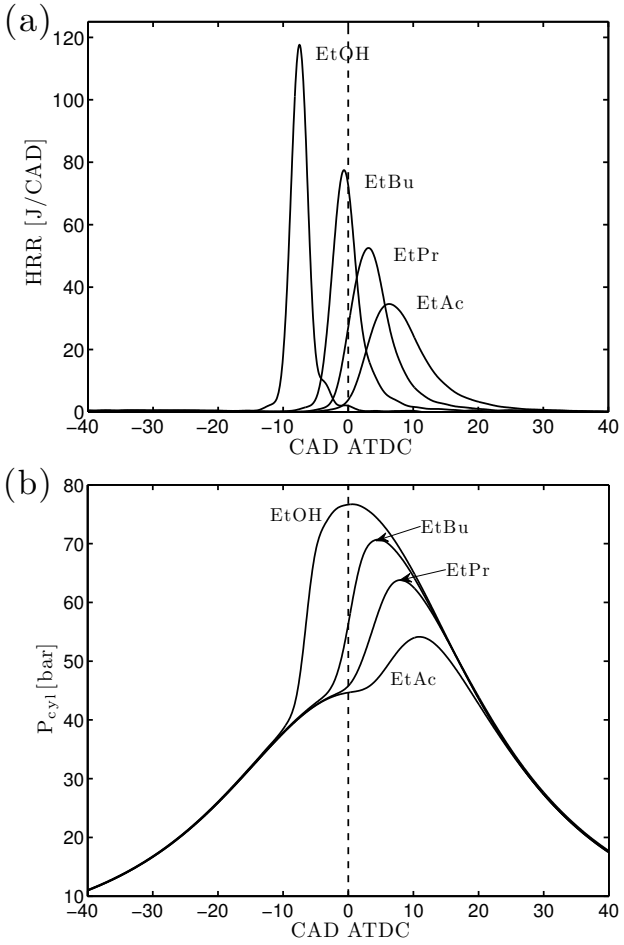

Figure 3: The heat release rate (a) and the pressure traces (b) for the four fuels at 1000 rpm and an equivalence ratio of 0.24.

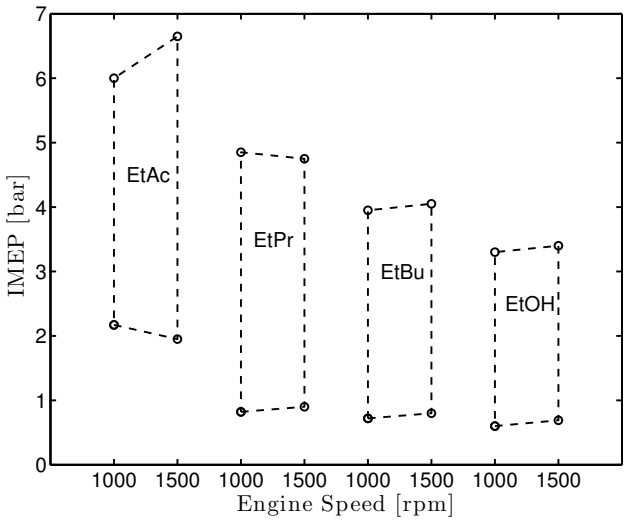

Figure 4: HCCI zones for the four fuels.

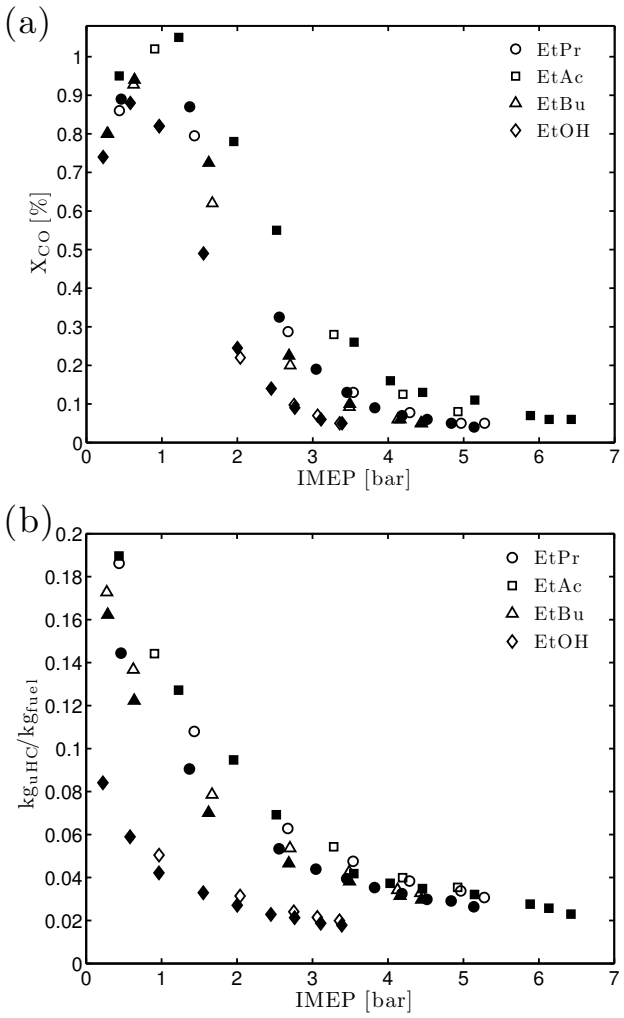

Figure 5: CO (a) and uHC (b) emissions for the fours fuels at 1000 rpm (empty symbols) and 1500 rpm (full symbols).

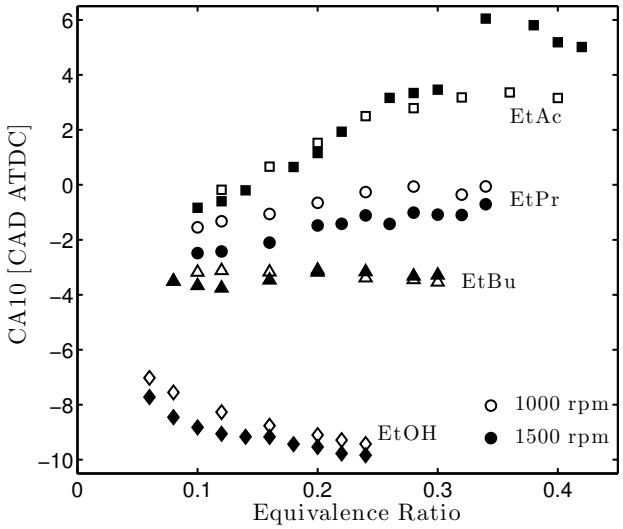

Figure 6: CA10 is used to estimate the ignition timing for the four fuels at 1000 rpm (empty symbols) and 1500 rpm (full symbols).

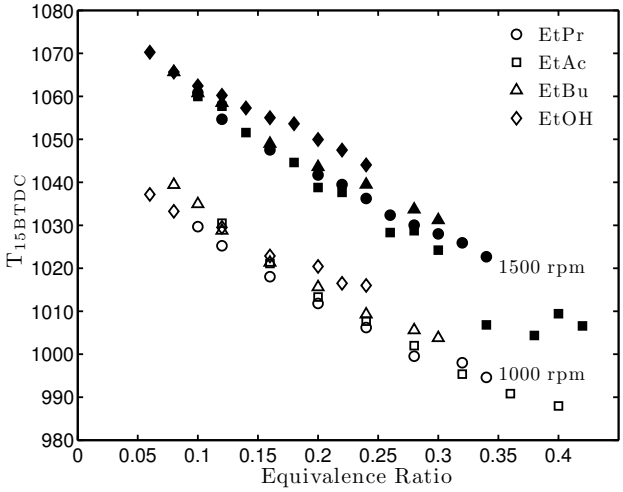

Figure 7: Temperature before ignition, here at 15 CAD BTDC for the four fuels at 1000 rpm (empty symbols) and 1500 rpm (full symbols).

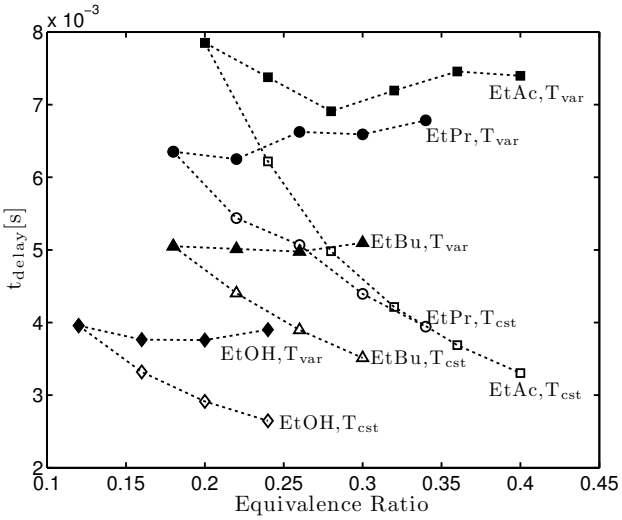

Figure 8: Ignition delays for temperatures not modified (empty symbols) or modified (full symbols) with equivalence ratios and based on the computed mass-averaged temperature at 15 CAD BTDC.

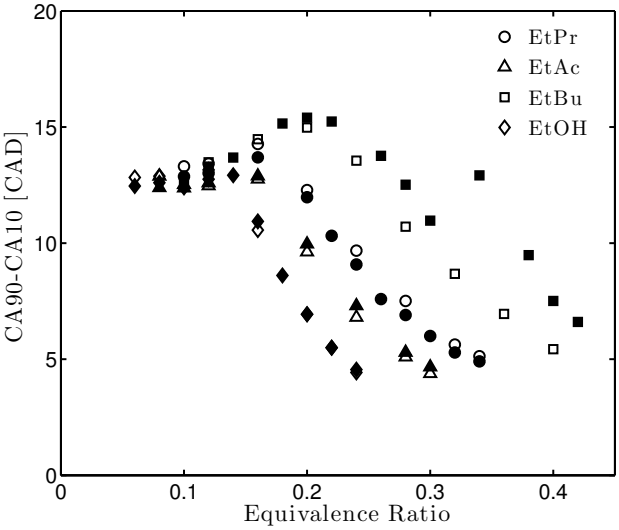

Figure 9: The combustion duration, calculated by CA90-CA10 for all fuels at 1000 rpm (empty symbols) and 1500 rpm (full symbols).